Journal of Fluorescence (2019) 29:599–607
https://doi.org/10.1007/s10895-019-02371-7

ORIGINAL ARTICLE

A Fluorescent Flavonoid for Lysosome Imaging: the Effect of Substituents on Selectivity and Optical Properties

Keti Assor Bertman[1] · Chathura S. Abeywickrama[1] · Ashley Ingle[1] · Leah P. Shriver[1,2] · Michael Konopka[1] · Yi Pang[1,3]

Received: 1 February 2019 / Accepted: 19 March 2019 / Published online: 6 April 2019

Abstract

Lysosome selective bright orange-red emitting flavonoid (**2**) was synthesized by attaching a strong donor (NPh_2) group into flavonoid skeleton. As a result of efficient intra molecular charge transfer due to the strong donor group, a significant bathochromic shift was observed from the emission of **2b** (with a $–NPh_2$ group, $\lambda_{em} \approx 590$ nm), in comparison that of **1b** (with a $–NMe_2$ group, $\lambda_{em} \approx 519$ nm). The role of the substituent effect towards ICT was further studied by low temperature spectral analysis. Fluorescence spectra at low temperature confirmed that large Stokes shift for probe **2** ($\Delta\lambda \approx 150$ nm) was due to strong ICT. Probe **2b** exhibited exceptional selectivity towards cellular lysosomes in live cells studies thus generating bright orange-red emission upon localization. Intra-cellular pH analysis results confirmed that probe **2b** did not participate in the elevation of lysosomal pH upon staining with different probe concentrations (0.5 μM – 2.0 μM) which is a potential advantage compared to acidotropic commercial LysoTracker® probes. This study further illustrated that the substituents in probe **2** play a significant role towards probe's organelle selectivity since probe **2a** (R = OH) did not show any lysosomal localization compared with **2b**. In addition, the calculated cytotoxicity data further revealed that this new probe design is highly biocompatible ($LC_{50} > 50$ μM) and suitable for long term imaging.

Keywords Excited state intra-molecular proton transfer (ESIPT) · Intra-molecular charge transfer (ICT) · Stokes shift · Flavonoid · Substituent effect · Lysosome probes

Introduction

Small molecule fluorescent probes have been widely used in fluorescence microscopy, as their applications facilitate visualization of intracellular components. [1, 2] Though fluorescence microscopy is a powerful tool, there are certain requirements that an ideal probe must meet, in order to apply it for bio-imaging studies. A reliable fluorescent probe should be (1) biocompatible, (2) highly selective to the organelle of interest, (3) readily excitable with existing microscope lasers, and (4) exhibit a large Stokes shift which minimizes possible spectral overlap. Many interesting fluorescent probes that have been developed due to increasing demand in the field. [1, 3] Flavonoids are a class of interesting molecules that have been recently used for bio-imaging applications. [4–7] The design and synthesis of flavonoid-containing probes have attracted more attention recently, due to their high biocompatibility and cell penetration ability. Their potential antioxidant, antiviral, anti-inflammatory, anti-cancer and anti-bacterial properties have also led to use these class of compounds in drug discovery and development. [8–12] Flavonoids exhibit a characteristic large Stokes shift, due to their ability to undergo excited state intramolecular proton transfer (ESIPT) and intramolecular charge transfer (ICT). In addition, the observed bright fluorescence emission due to rigid fluorophore skeleton brings further attention to the use of flavonoid skeleton in fluorescent sensor development. One of the major limitations in current flavonoid-based probe design is that their emissions occur at shorter wavelengths, often limited to the green region.

Electronic supplementary material The online version of this article (https://doi.org/10.1007/s10895-019-02371-7) contains supplementary material, which is available to authorized users.

✉ Yi Pang
yp5@uakron.edu

[1] Department of Chemistry, University of Akron, Akron, OH 44325, USA

[2] Department of Biology, University of Akron, Akron, OH 44325, USA

[3] Maurice Morton Institute of Polymer Science, University of Akron, Akron, OH 44325, USA

In addition to the extension of molecular conjugation, ESIPT and ICT are effective mechanisms to generate a bathchromic shift in flavonoid emission. However, their relative contribution towards emission is not well understood in tuning flavonoid emission.

Lysosomes are membrane-bound acidic organelles (pH ≈ 5.0) participating in an extensive number of dynamic cellular activities. [13, 14] The main function of lysosomes is to degrade and recycle biomacromolecules. Lysosome tracking in live cells enables us to understand real-time dynamics such as lysosomal distribution and morphology which directly related to cellular health. Some commercial lysosome probes such as LysoTracker® Blue DND-22 (λ_{abs}~373 nm, λ_{em}~422 nm, Δλ~49 nm), LysoTracker® Green DND-26 (λ_{abs}~504 nm, λ_{em}~511 nm, Δλ~7 nm) are often used for lysosome visualization. However, they suffer from small Stokes shift (Δλ <20 nm) which limits their application in fluorescent microscopy. Additionally, commercial probes such as LysoTracker® Red DND-99 (λ_{abs}~577 nm, λ_{em}~590 nm, Δλ~13 nm), LysoTracker® Deep Red (λ_{abs}~647 nm, λ_{em}~668 nm, Δλ~21 nm) are available with enhanced excitation/emission properties. Moreover, all commercial LysoTracker® probes consist of basic primary or secondary amino groups which could elevate internal lysosomal pH via "alkalinizing effect". The potential toxicity arises due to the characteristic "alkalinizing effect" of such commercial probes, which limits their application in time-dependent experiments. Therefore, the development of photophysically improved and highly biocompatible fluorescent probes for lysosome visualization remains a challenge.

Our recent study reported the bright green-emitting, highly biocompatible flavonoid derivative **1b** which exhibited exceptional selectivity toward lysosomes in living cells (Scheme 1). [15] Despite the presence of a morpholine group, **1b** appeared to be non-toxic, and its application did not induce intracellular pH change. In order to improve the photophysical characteristics of **1**, it might be interesting to examine probe **2** that includes a strong donor group (i.e., diphenylamine) (Scheme 1). As seen from the structure of **2**, the substituent on the C-ring *could* play pivotal role to influence the optical property, since **2a** allows both ESIPT and ICT, while **2b** only permit ICT interaction. Another intriguing question is whether the substitution will affect probe's lysosome selectivity. Herein, we describe the synthesis and optical properties of **2.** The results show that **2** exhibited bright orange emission (λ_{em}~600 nm) with a large Stokes shift (Δλ~200 nm) due to strong intra-molecular charge transfer (Scheme 1) while retaining the desirable selectivity towards intracellular lysosomes. In addition to bright orange-red emission upon localization in cellular lysosomes, **2b** also exhibited high biocompatibility and environmental sensitivity for wash-free staining application (i.e., no post staining washing is required before imaging), showing significant impact from the substituent.

Materials and Methods

All solvents and reagents were used as received without further purification unless specified otherwise. Reactions were performed under standard atmosphere conditions in oven-dried glassware. All molecular biology grade reagents for cell culture and fluorescent confocal microscopy were purchased from Fisher Scientific. UV-vis spectra were obtained with Hewlett Packard-8453 diode array spectrophotometer at 25 °C. Fluorescence spectra were measured with HORIBA Fluoromax-4 spectrofluorometer. ^{1}H NMR spectra were obtained on a Varian 300 MHz spectrometer in deuterated dimethyl sulfoxide (*d*-DMSO) or chloroform ($CDCl_3$) solvents. Fluorescence confocal laser microscopy imaging was performed in Nikon A1 system with 60x or 100x oil objective. Commercial LysoTracker® Green DND-26 was excited with 488 nm laser line, and emission was collected in the range 495–550 nm range. Probe **2a** and **2b** were excited with 405 nm laser line and emissions were collected in the range 570–700 nm.

Note: Co-localization experiments were conducted with laser lines in multiple tracks cautiously to avoid any possible background interferences. No background fluorescence signal was obtained for LysoTracker® Green with 405 nm laser line.

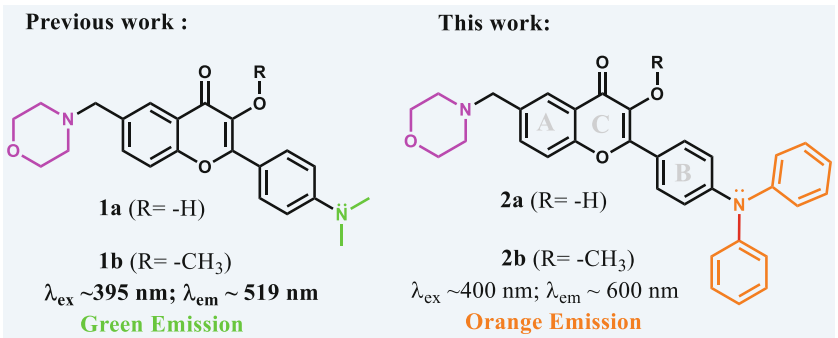

Scheme 1 Chemical structures of flavonoids **1** and **2**, and the optical properties of **1b** and **2b** (in EtOH)

Synthesis

Probes **2a** and **2b** were synthesized according to the previously reported procedure. [15]

General Procedure for 2a

In a 50 ml round bottom flask, 1.1 mmol of 4-(diphenylamino)benzaldehyde was dissolved in 35 mL of ethanol. Then 2-hydroxy-5-(morpholinomethyl)acetophenone (1.0 mmol) was added and the resulting dark brown solution was heated up and stirred at 45^0 C for 5 min to completely dissolve the solid. Then aqueous potassium hydroxide (7 mmol) was slowly added while the solution was on ice. Once the solution was stirred for 5 h, the reaction was heated up to 50^0 C for 10 additional hours. Upon completion, the orange color solution was then cooled down again to 0^0 C and another 7 mmol portion of potassium hydroxide was added. To the resulting dark orange solution, aqueous H_2O_2 solution (2 mL of 30%) was slowly added. After 12 h, the reaction mixture was neutralized on ice and concentrated under the vacuum to obtain an orange color solid.

2-(4-(Diphenylamino)phenyl)-3-hydroxy-6-(morpholinomethyl)-4H-chromen-4-one **(2a)** was obtained as a dark orange color solid; ^{1}H NMR (DMSO-*d*, 300 MHz) δ 2.36 (t, 4H), δ 3.57 (s, 6H), 7.04 (d, 2H), δ 7.12 (t, 6H), δ 7.35 (m, 4H), δ 7.69 (s, 2H), δ 7.95 (d, 3H), and 9.46 (s, 1H). HRMS (ESI) found (m/z) for [M+] 543.1680, 544.1801, 545.1931 and 546.1984. Calculated (m/z) were 543.1686, 544.1686, 545.1686 and 546.1686.

Synthesis of 2b

To a 50 ml round bottom flask **2a** (1 mmol), 10 mL of Me_2SO_4, K_2CO_3 (4 mmol), and excess of $MgSO_4$ were added and mixed thoroughly for 24 h at room temperature. Upon completion, the mixture was allowed to settle for 10 min and filtered. The filtrated was then mixed with 1 M NaOH to degrade the dimethyl sulfate. Then the precipitated yellow crude was collected by vacuum filtration. The desired product, **2b**, was further purified on a column chromatography that is packed with silica gel (in DCM).

2-(4-(Diphenylamino)phenyl)-3-methoxy-6-(morpholinomethyl)-4H-chromen-4-one **(2b)**. Was obtained as a dark orange color solid; ^{1}H NMR (DMSO-*d*, 300 MHz) δ 2.36 (t, 4H), δ 3.57 (s, 6H), δ 3.80 (s, 3H) 6.97 (d, 2H), δ 7.16 (t, 6H), δ 7.38 (t, 4H), δ 7.69 (m, 2H), δ 7.95 (d, 3H). HRMS (ESI) found (m/z) for [M+] 557.0671, 558.0919, 559.1003 and 560.1008. Calculated (m/z) were 557.1834, 558.1843, 559.1843 and 560.1843.

Table 1 Optical properties of **2a** and **2b**

Solvent	2a				
	λ_{abs} (nm)	λ_{em} (nm)	ϕ_{fl}	$\Delta\tilde{\nu}$ (cm^{-1})	(M^{-1} cm^{-1})
Toluene	409	475[a], 580[b]	0.57	7208	28,378
DCM	409	530[a], 590 [b]	0.55	7501	29,273
CH_3CN	400	510[a], 572[b]	0.19	7517	24,226
DMSO	404	540[a], 600[b]	0.27	8086	27,045
ETOH	406	590	0.05	7389	29,814
MEOH	403	540[a], 600[b]	0.24	8147	23,048
H_2O	406	597	0.01	7880	17,892
	2b				
Toluene	388	470	0.76	4497	20,843
DCM	393	530	0.61	6577	22,290
CH_3CN	385	560	0.41	8117	21,616
DMSO	393	560	0.35	7588	20,391
ETOH	397	587	0.04	8153	22,478
MEOH	397	603	0.01	8605	22,165
H_2O	392	575	0.18	8119	16,490

[a] Emission reported from normal form N^*

[b] Emission reported from tautomer form T^*

Live Cell Imaging

Fluorescent confocal microscopy imaging was performed on a Nikon A1 confocal system with 60 x and 100 × oil objective with a numerical aperture of 1.45 and a refractive index of 1.5. Imaging temperature was maintained at 37^0 C at all times. The excitation used for our dyes was 405 nm. Standard DAPI, FITC, and mCherry emission filters were used. All imaging was done in an Okolab Bold Cage Incubate or at 37 °C, and images were processed using NIS Elements or ImageJ Pro (NIH) imaging software.

Scheme 2 Synthesis of **2**

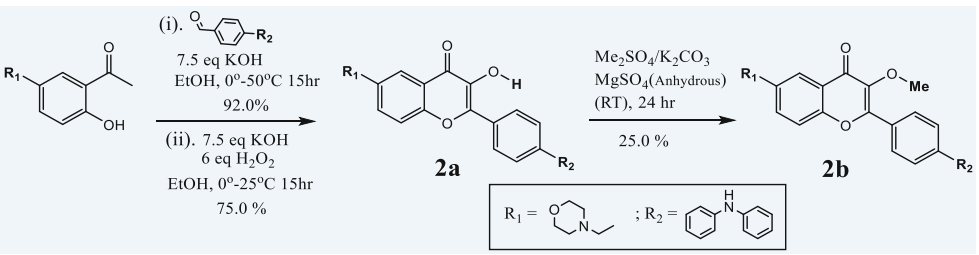

Cell Culturing and Staining

MO3.13 cells (progenitor oligodendrocytes) or NHLF (normal human lung fibroblast) cells were plated on Mat Tek 35 mm dish with glass bottom at a density of 1×10^5 cells per plate in DMEM media enhanced with 10% fetal bovine serum (Gibco) and 1% penicillin/streptomycin. Cells were incubated overnight at 37 °C and in 5% CO_2. Subsequent to incubation, cells were washed with 1× PBS and treated with 0.5 μM stain in Invitrogen™ Molecular Probes™ Live Cell Imaging Solution for 30 min. After treatment, cells were washed once for 1 min with 1 × PBS. Invitrogen™ Molecular Probes™ Live Cell Imaging Solution was added to cells for imaging. Lysotracker®, ER-Tracker™, or ER-Tracker™ stock solution was made in DMSO and total DMSO levels were maintained in the media below 0.5% (*V*/V%) All cells were maintained in a 5% CO_2 humidified atmosphere at 37 °C.

Cell Viability Assay

The viability of NHLF following treatment with **2a** and **2b** were evaluated using Biotium MTT assay. NHLF were plated in a 96 well plate at 7.3×10^4 cells/mL with DMEM 10% FBS and 1% penicillin/streptomycin and allowed to adhere overnight at 37 °C with 5% CO_2. Probe treatments, 0.14 μM–70 μM, or vehicle control, 0.5% DMSO, were dissolved in DMEM 10% FBS and 1% penicillin/streptomycin. Each treatment concentration was applied in triplicate, with the exception of vehicle control applied to 12 wells and incubated for 24 h. After24 hours, media and treatment were aspirated and replaced with DMEM 10% FBS and 1% penicillin/streptomycin containing 0.1 mg/mL MTT and incubated for 3.5 h at 37 °C. Plates were centrifuged at 1000 x g for 10 min, following which media was carefully aspirated and replaced with MTT solvent, prepared according to MTT manufacturer's instruction. From this point, plates were protected from light and placed on a shaker for 15 min. Absorbance values were read at 570 nm with a reference at 630 nm. Percent viability was determined by the following (treatment absorbance) / (average vehicle control absorbance) × 100. Dose response curves and statistics were generated using GraphPad Prism 5 software.

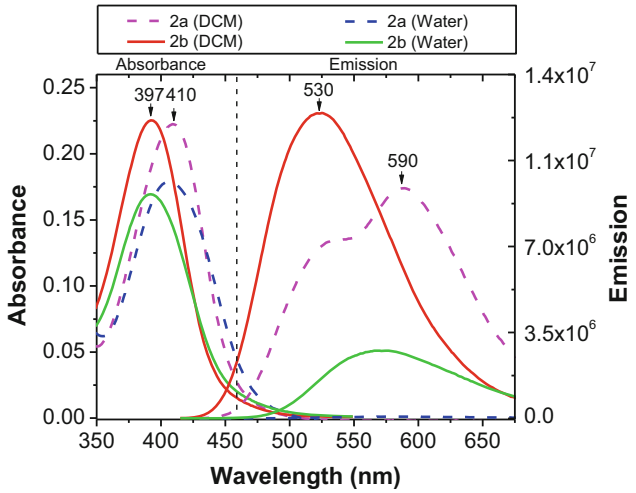

Fig. 2 A summary of spectroscopic properties of probes **2a** and **2b** in DCM and water. Absorbance and emission data were obtained with 1 μM probe concentration at 25 °C. Probes **2a** and **2b** were excited at 400 nm

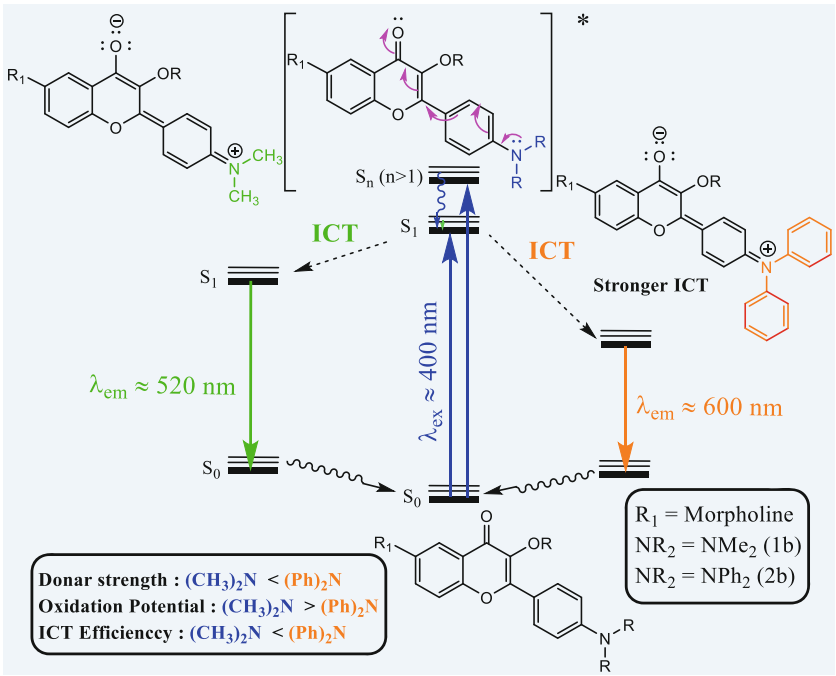

Fig. 1 Comparison of the ICT process in **1b** and **2b**

Intra-Cellular pH Determination

NHLF (normal human lung fibroblast) cells were plated on Mat Tek 35 mm dish with glass bottom at a density of 4×10^4 cells per plate in DMEM media enhanced with 10% fetal bovine serum (Gibco) and 1% penicillin/streptomycin. Cells were incubated overnight at 37 °C and in 5% CO_2. Subsequent to incubation, cells were washed with 1× PBS and treated with 0.5 μM, 1 μM, and 2 μM probe (**2a** or **2b**) concentration and incubated at 37^0 C for 30 min. Then cells were washed three times with 1x PBS and treated with 5 μg/ml pHrodo™ Red Avidin fluorogenic pH sensor for 1 h at 0^0 C. Then cells were further incubated for 30 min at 37^0 C. After treatment, cells were washed three times with 1 × PBS and Invitrogen™ Molecular Probes™ Live Cell Imaging Solution was added to cells for imaging. Cells were analyzed by fluorescent confocal microscopy. Probes **2a** and **2b** were excited with 405 nm laser and pHrodo™ Red Avidin was excited with 561 nm laser. All microscope parameters (including power, gain, magnification) were kept constant for pHrodo™ Red Avidin imaging. Obtained fluorescent images were analyzed by ImageJ (NIH) software and colocalized regions were identified for all probe concentrations. Average fluorescent intensity of the red channel (pHrodo) was calculated for randomly selected colocalized regions and bar-chart was generated based on results.

Fluorescence Quantum Yield

The fluorescence quantum yields (ϕ_{fl}) for compounds were calculated by using quinine sulfate (Sigma) as the standard ($\phi_{ref} = 0.54$, ethanol) at 370 nm. The following equation was used for calculation.

$$(\phi_{fl})sample = \phi_{Ref} \times \frac{Abs_{Ref}}{Abs_{Sample}} \times \frac{I_{Sample}}{I_{Ref}} \times \frac{(\eta_{Ref})^2}{(\eta_{Sample})^2}$$

Where Abs is the absorbance of the sample, I is the integrated fluorescence emission intensity and η is the refractive index of the solvent.

Results and Discussion

Synthesis

Probes **2** were synthesized via Claisen-Schmidt condensation and Algar-Flynn-Oyamada reaction as described in the previous report (Scheme 2). [15] The resulting crude product **2a** and **2b** were further purified on a silica gel column with methylenedichloride and ethyl acetate (8:2), characterized by

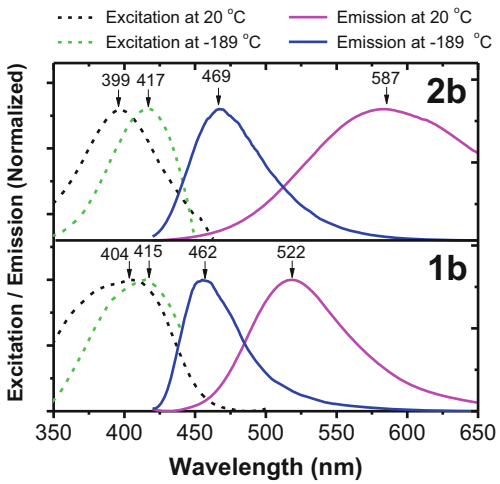

Fig. 3 Low temperature vs. room temperature spectroscopic data obtained for probes **2b** (top) and **1b** (bottom) in ethanol (1×10^{-6} M probe concentration)

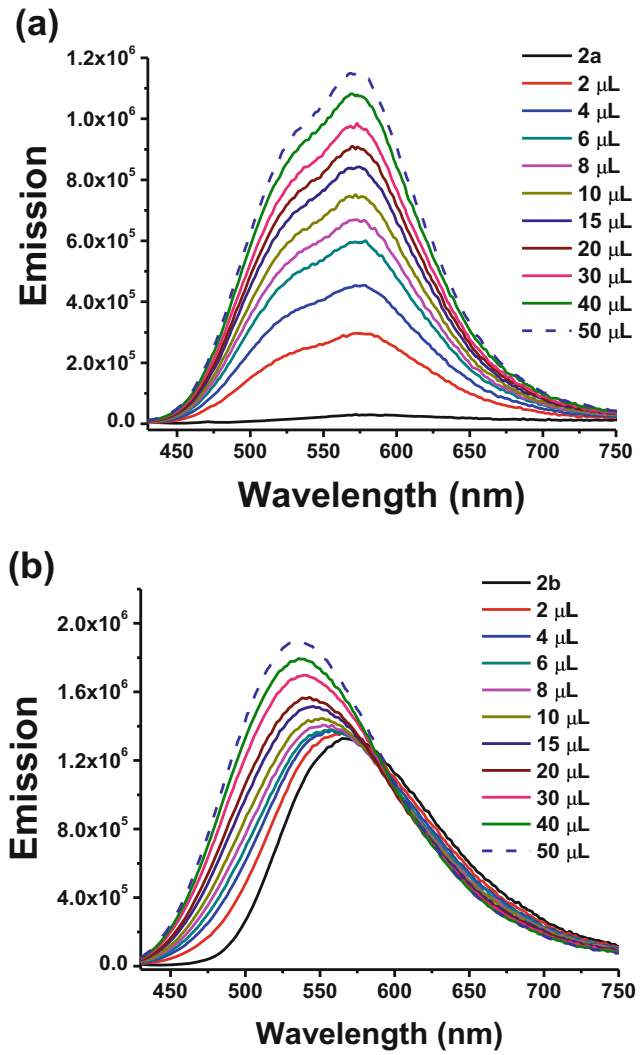

Fig. 4 Fluorescence response of **2a** (**a**) and **2b** (**b**) in de-ionized water (5×10^{-6} M) upon titration with 10% BSA (*w/v*) at room temperature

using ^{1}H NMR spectroscopy and high-resolution mass spectrometry (ESI **S1**–**2**).

Spectroscopic Properties

Spectroscopic properties of **2a** and **2b** were studied in different solvents (Fig. 2 and Table 1). Similar absorption peaks were observed from **2a** ($\lambda_{abs} \approx 410$ nm) and **2b** (($\lambda_{abs} \approx 397$ nm), which were only slightly affected by solvent polarity. However, the emission exhibited a significant bathochromic shift ($\Delta\lambda \approx 60$ nm in DCM) from **2b** ($\lambda_{em} \approx 530$ nm) to **2a** ($\lambda_{em} \approx 590$ nm). The observed large spectral shift could be attributed to the coupling of excited state intramolecular proton transfer (ESIPT) with intra-molecular charge transfer (ICT) process, due to the presence of the hydroxyl group (R = OH) in **2a**. Probes exhibited significantly larger Stokes shifts in all solvents ($\Delta\lambda \approx 130$–$180$ nm).

It is important to notice that emission of **2** occurred at a significantly longer wavelength (Scheme 1), in comparison with that of **1** ($\lambda_{abs} \approx 385$–$403$ nm, $\Delta\lambda \approx 60$–80 nm).[8] Clearly, the diphenylamine group in **2** acts as a stronger donor group in comparison with dimethylamine moiety in **1**, inducing a stronger ICT process in the former (Fig. 1). The assumption is consistent with the oxidation potential of the donor group (where E_{ox} $Me_2N > E_{ox}$ Ph_2N). [16] The evidence of the substituent impact was further revealed from a spectroscopic comparison between **1b** and **2b** (Scheme 1), as their emission characteristics will be determined mainly by ICT (without the impact from ESIPT). Although the donor group is expected to have some impact on the conjugation length of the probes, no significant changes were observed in the absorption spectra of **2b**, in comparison with **1b** (Fig. 2). However, probe **2b** showed a noticeable solvatochromic effect ($\lambda_{em} \approx 530$ in DCM; $\lambda_{em} \approx 575$ in H_2O) over a range of different solvents and exhibited higher fluorescent quantum yield (ϕ_{fl}) across all solvents examined (including water). Spectroscopic study with higher concentrations of **2b** in water did not reveal any signs of aggregation (ESI 3).

Low-Temperature Spectroscopic Studies In order to verify the role of the donor group in the observed bathochromic shift ($\Delta\lambda \approx 60$–80 nm from **1b** to **2b**), low temperature fluorescence spectra were acquired in ethanol. Samples of **1b** and **2b** in EtOH were frozen to −189 °C in liquid nitrogen to limit the molecular motion and bond reorganization that are associated with the ICT process. At −189 °C, very similar emission was observed from **1b** ($\lambda_{em} = 462$ nm) and **2b** ($\lambda_{em} = 469$ nm) (Fig. 3). Very similar emission wavelength and profiles observed from **1b** and **2b** at −189 °C pointed to that both **1b** and **2b** had similar locally excited states in the initial excitation process, as ICT process was frozen. When the temperature was gradually raised to room temperature, a significant

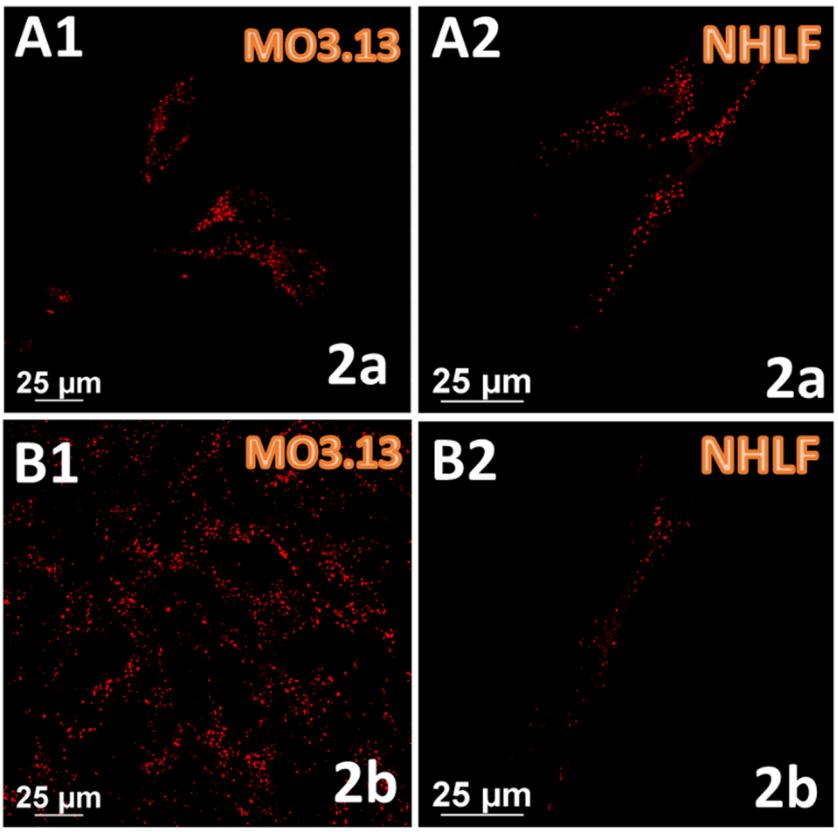

Fig. 5 Images for **2a** red channel in two different cell lines (A1 in MO3.13 and A2 in NHLF) and **2b** red channel (B1 in MO3.13 and B2 in NHLF) at 60x, after incubation at 0.5 µM for 30 min. Probes were excited at 405 nm and Texas Red filter was used as described in the method section

difference was observed from the probe emissions (**1b** vs. **2b**). However, the excitation spectra of probe **1b** and **2b** did not show such significant change as the temperature was raised. Therefore, the observed large difference in the emission of **1b** and **2b** was attributed to the stronger ICT in the latter, as ammonium [Ph_2N^+] is more stable cation than [Me_2N^+].

Spectrometric Titrations with Bovine Serum Albumin (BSA)

Spectrometric titrations were conducted for **2a** and **2b** in the presence of 10% BSA (w/v in water). Significant fluorescent enhancement was observed from probe **2a** upon addition of BSA (Fig. 4a), in sharp contrast to slightly increment from **2b** (Fig. 4b). The fluorescence enhancement upon BSA binding was ≈ 40 times for probe **2a**, after the addition of 50 μL of 10% BSA. The absorption spectra of probes **2a** and **2b** did not show any change upon addition of BSA (ESI Fig. **S10**). A large difference between **2a** and **2b** in responding to BSA proteins indicated that the substituent played a significant role in affecting the probe's ability to internalize into the hydrophobic pocket of proteins.

Live Cell Study

Probes **2a** and **2b** were further examined to investigate their potential use in live cell imaging applications. Normal human lung fibroblast (NHLF) and progenitor oligodendrocytes (MO3.13) cells were stained with probes **2a** and **2b** (500 nM) for 30 min and studied under the fluorescent confocal

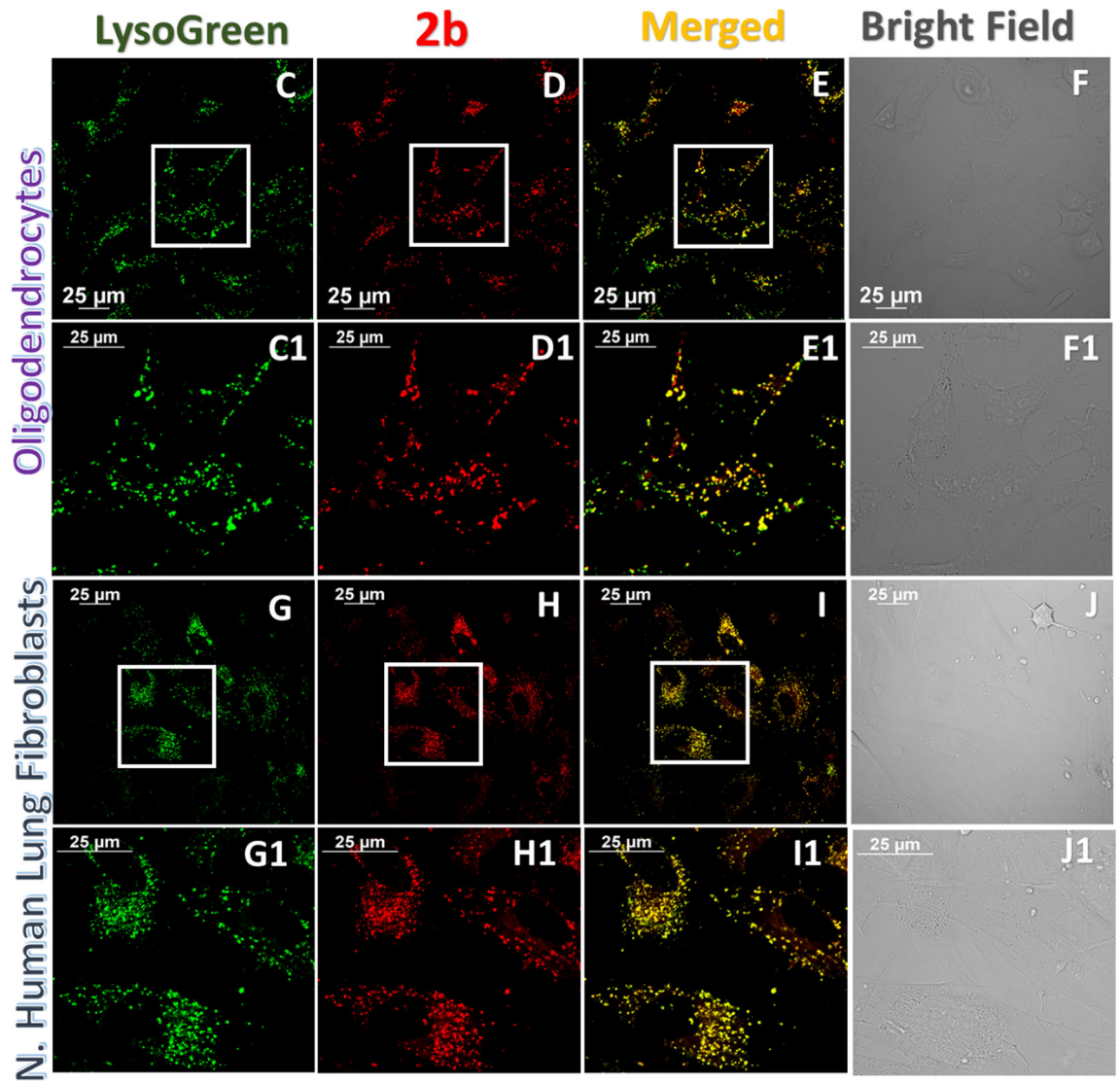

Fig. 6 Fluorescent confocal microscopy images of MO3.13 and NHLF cells (×60) treated with **2b** (0.5 μM) for 30 min. Images show in C, D, E, F the MO3.13 fluorescence images at 60x of LysoTracker Green®, **2b**, merged channels and bright field, respectively. Images in C1, D1, E1, F1 are the digitally enlarged images of C, D, E, F in the selected area. Images show in G, H, I, J the NHLF fluorescence images at 60x of LysoTracker Green®, **2b**, merged channels and bright field, respectively. Images in G1, H1, I1, J1 are the digitally enlarged images of G, H, I, J in the selected area. Laser 488 nm and 405 nm were used for the green and red channels, respectively

microscope. Interestingly, the initial staining of **2a** and **2b** exhibited excellent internalization by generating non-uniform fluorescence emission pattern throughout the stained cells (Fig. 5 and ESI **S4**). Colocalization with commercial LysoTracker Green® DND-26 showed nearly identical staining patterns for both probe **2b** and LysoTracker® Green confirming lysosome selectivity of the probe **2b** in both cell lines (Fig. 6). Calculated Mander's overlap coefficient for probe **2b** in the presence of the LysoTracker® Green was above 0.95 in NHLF (ESI **S5**) which further confirmed its exceptional lysosome selectivity. Surprisingly probe **2a** did not show any lysosomal specificity in colocalization experiments (ESI **S6**). It is quite interesting that the difference between probe **2a** and **2b** solely depended on the protection of the hydroxyl group in the structure. However, the observed results indicated a sharp contrast with our previously reported flavonoid models (**1a** and **1b**) where excellent lysosome colocalization was observed for both **1a** and **1b** in the presence of with LysoTracker® Red. Even though probe **2a** consists of a lysosome directing morpholine moiety, it showed only a slight overlap with LysoTracker® Green in NHLF cells, with the Mander's colocalization coefficient calculated was 0.35 (ESI **S5**), which statistically eliminated the lysosome selectivity of **2a**. In other words, the protection of the hydroxyl group was necessary to maintain the desired lysosome selectivity, as observed from **2b**. Colocalization studies conducted to identify the possible localization of probe **2a** was unsuccessful where probes **2a** and **2b** did not show any selectivity towards organelles such as ER and mitochondria (ESI **S10**–**11**).

To determine the effect of **2b** towards possible pH elevation within cellular lysosomes (i.e., alkalinization), we analyzed the pH change in the lysosome in the presence of different concentrations of probe **2b** (0.5–2 μM) in NHLF by using fluorogenic pHrodo™ Red Avidin. (Fig. 7a, ESI **S7**-**S9**). Interestingly, probe **2b** did not show any signs of pH elevation, as the detected fluorescence response from pHrodo™ Red Avidin remained consistent over a range of different concentrations of **2b** (Fig. 7a). In addition, cell viability experiments were performed, by MTT cell proliferation viability assay which showed the calculated LC_{50} for probe **2b** > 50 μM (Fig. 7b). The results thus illustrated two significant advantages of probe **2b** over existing commercial LysoTracker® probes: (i) high biocompatibility, benefitting from the flavonoid structure; and (ii) its non-alkalinizing nature when applied in to live cell experiments. These properties pointed to that probe **2b** could be used as a potentially useful tool for visualization of lysosomes in live cells, especially for long term imaging sessions where cytotoxicity is a major concern.

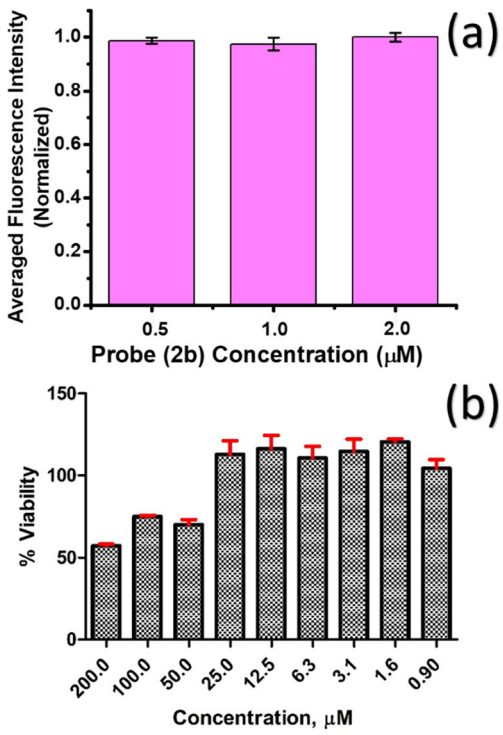

Fig. 7 **a** Calculated average fluorescence intensity obtained from pHrodo™ Red Avidin upon treatment with different concentration of probe **2b** (0.5–2 μM) in NHLF. **b** Cell viability results obtained for **2b**, MTT Cell Proliferation Assay

Conclusions

In conclusion, flavonoid-based fluorescent probes **2a** and **2b** were synthesized by attaching a strong donor Ph_2N- group. Probes **2a** and **2b** exhibited a large Stokes shift (150–200 nm) due to the integrated ICT and ESIPT process. By using low-temperature fluorescence, the contribution of ICT towards bathochromic spectral shift is estimated to be ≈ 118 nm from **2b**, which is significantly larger by ≈60 nm observed from the analog **1a** (with a Me_2N- group). The study indicated that a Ph_2N- substituent can induce a larger ICT interaction compared Me_2N- group in flavonoid compounds, generating a significant bathochromic shift in emission. Probe **2b** (R = OMe) exhibited an exceptional selectivity towards cellular lysosomes where bright orange-red fluorescence was observed upon localization. In sharp contrast, probe **2a** (with a –OH substituent) does not show any lysosomal localization, illustrating the importance of the substituents towards the selectivity. Attractively, probe **2b** has very low toxicity (LC50 > 50 μM) and does not show any noticeable pH elevation in live cells with different concentrations. Therefore, probe **2b** could be a potentially useful probe for lysosome imaging.

Acknowledgments We acknowledge partial support from Coleman Endowment from The University of Akron. We thank Nicolas Alexander from The University of Akron for acquiring mass spectra data. We also thank Hannah J Baumann from The University of Akron for conduction MTT cell viability assays. The NHLF cell line was a kind gift from Dr. Sailaja Paruchuri at The University of Akron.

References

1. Johnson I, Spence MTZ (2010) The handbook: a guide to fluorescent probes and labeling technologies
2. Zhang J, Campbell RE, Ting AY, Tsien RY (2002) Creating new fluorescent probes for cell biology. Nat Rev Mol Cell Biol 3:906–918
3. Wiederschain GY (2011) The molecular probes handbook. A guide to fluorescent probes and labeling technologies. Biochem 76:1276–1276
4. McDonald L, Liu B, Taraboletti A, Whiddon K, Shriver LP, Konopka M, Liu Q, Pang Y (2016) Fluorescent flavonoids for endoplasmic reticulum cell imaging. J Mater Chem B 4:7902–7908
5. Liu B, Shah M, Zhang G, Liu Q, Pang Y (2014) Biocompatible flavone-based fluorogenic probes for quick wash-free mitochondrial imaging in living cells. ACS Appl Mater Interfaces 6:21638–21644
6. Havsteen BH (2002) The biochemistry and medical significance of the flavonoids
7. Zhao C, Liu B, Bi X, Liu D, Pan C, Wang L, Pang Y (2016) A novel flavonoid-based bioprobe for intracellular recognition of Cu2+ and its complex with Cu2+ for secondary sensing of pyrophosphate. Sensors Actuators B Chem 229:131–137
8. Pietta PG (2000) Flavonoids as antioxidants. J Nat Prod 63:1035–1042
9. Hertog MGL, Feskens EJM, Kromhout D, Hertog MGL, Hollman PCH, Hertog MGL, Katan MB (1993) Dietary antioxidant flavonoids and risk of coronary heart disease: the Zutphen elderly study. Lancet 342:1007–1011
10. Litvinov VP (2007) Chemistry and biological activities of 1,8-naphthyridines. Russ Chem Rev 73:637–670
11. Chahar MK, Sharma N, Dobhal MP, Joshi YC (2011) Flavonoids: a versatile source of anticancer drugs. Pharmacogn Rev 5:1–12
12. Cushnie TPT, Lamb AJ (2005) Antimicrobial activity of flavonoids. Int J Antimicrob Agents 26:343–356
13. Cooper G (2000) The Cell: A Molecular Approach, 2nd ed. Sinauer Associates, Sunderland (MA)
14. Chen X, Bi Y, Wang T, Li P, Yan X, Hou S, Bammert CE, Ju J, Gibson KM, Pavan WJ, Bi L (2015) Lysosomal targeting with stable and sensitive fluorescent probes (superior LysoProbes): applications for lysosome labeling and tracking during apoptosis. Sci Rep 5:9004–9013
15. Bertman KA, Abeywickrama CS, Baumann HJ, Alexander N, McDonald L, Shriver LP, Konopka M, Pang Y (2018) A fluorescent flavonoid for lysosome detection in live cells under "wash free" conditions. J Mater Chem B 6:5050–5058
16. Novakova V, Hladík P, Filandrová T, Zajícová I, Krepsová V, Miletin M, Lenčo J, Zimcik P (2014) Structural factors influencing the intramolecular charge transfer and photoinduced electron transfer in tetrapyrazinoporphyrazines. Phys Chem Chem Phys 16:5440–5446